Oscillating Arc as an Improvement Strategy for Welds in Thermal Storage Systems in CSP Plants

Luis Guerreiro [1], Raúl Pasten [2], Mauro Henriquez [2], Juan Reinoso-Burrows [2], Carlos Soto [2] and Carlos Duran[2]

[1] *ICT-Institute for Earth Sciences, Univ. Evora,* IIFA, Palacio Vimioso, 7002 Evora, Portugal

[2] *Centro de Desarrollo Energético Antofagasta (CDEA),* Av. Universidad de Antofagasta 02800, Antofagasta, Chile

Abstract

The molten salt two-tank thermal storage system, based on a mixture of sodium nitrate and potassium, is widely used in concentrating solar power plants, operating between 290 °C and 565 °C. However, failures associated with the welded joints have been reported. This study evaluates the effect of oscillated arc versus non oscillation arc on welds exposed to molten salts. Techniques such as electron microscopy, metallography, microhardness and dilution analysis were applied to characterize the microstructure after different exposure times. The results indicate that arc oscillation improves the distribution of protective elements, reduces residual stresses and decreases mass loss under severe conditions.

Keywords: Renewable electricity, Capacity installed, Storage, Thermal Energy Storage (TES)

1. Introduction

Solar tower concentrated solar power (CSP) plants use two-tank thermal storage systems for molten solar salts: one "cold" salt tank and one "hot" salt tank. In the case of parabolic trough technology, the cold salt tank typically operates at temperatures ranging from 290°C to 393°C [1] since the plants usually make use of a synthetic oil which degrades at 400ºC and is the heat transfer fluid of the primary solar loop. In tower technology, the hot salt tank can reach temperatures of up to 565°C in commercial plants like the one of Torresol located near Seville, Spain. The capacity of these tanks is directly related to the plant's installed power, allowing for the storage of thousands of tons of solar salts with tanks as high as 15 meters. This system ensures energy supply during periods without solar radiation, maximizing the continuous operation of the plant. The thermal energy storage (TES) system is a fundamental component of concentrated solar power (CSP) plant technology [2]. Currently, the most commonly used material in solar thermal plants is solar salt (60% $NaNO_3$ + 40% KNO_3) [3], [4], [5].

Regarding the materials used in tank construction, they are designed to withstand the thermal high temperatures and thermal stress and also the chemical conditions imposed by molten salts. For hot salt tanks, stabilized stainless steels such as AISI 347H and AISI 321H are used, offering high corrosion resistance at elevated temperatures [6][7]. On the other hand, cold salt tanks are typically made of carbon steel ASTM A516 Gr-70 or stainless steels such as AISI 304. These materials have been selected in order to ensure a good operation from the structural and also that there is no leakage for the whole service life under the demanding operational conditions of CSP plants. [8], [9]. Stainless steel tanks are additionally insulated with mineral wool, refractory bricks, or ceramic materials that can withstand the high temperatures of up to 600ºC. Due to their large dimensions, these systems are welded on-site at the plant [10][11]. The tanks are equipped with piping systems

10.18086/swc.2025.01.15 Available at http://proceedings.ises.org

for the inlet and outlet of molten salts, pumps, and high-pressure valves capable of withstanding extreme temperatures up to 600ºC. The tanks typically have a flat bottom and a dome-shaped cover. The floor and shell thicknesses are designed with minimum values based on the API 650 standard. Although there is not yet a specific technical standard for the design of TES tanks with molten salts, current tanks are designed according to API 650 and ASME Section II standards, which are limited for the high temperatures and conditions of TES tanks with molten salts.

Although molten salts have been successfully used in parabolic trough plants, failures have been reported in the tanks of central receiver plants, causing significant economic losses and skepticism about the technology [8]. These failures are related to the early stage of the technology and issues in design, manufacturing, commissioning, and operation. A representative example is the CSP Crescent Dunes project in the United States[12]. The problems associated with the molten salt tank in this project included issues such as corrosion, operational reliability, thermal stress, maintenance challenges, and cost implications. These problems highlight the importance of meticulous design, proper selection of materials and rigorous welding quality assurance procedures, which are critical for a successful performance.

Currently, the most commonly used welding processes in such two tank system are gas metal arc welding (GMAW) and gas tungsten arc welding (GTAW), which require careful quality control to minimize these defects and ensure durability [8], [13], [14].
The current investigation is being carried out in order to evaluate the influence of mechanical arc oscillation on welding beads using the GMAW process with short-circuit metal transfer in a high-temperature molten salt medium.

2. Methodology

This research examines the influence of mechanical arc oscillation on the morphology, dilution, and metallurgical characteristics of weld beads produced by the Gas Metal Arc Welding (GMAW) process. Comparative analyses were performed between welds carried out with and without oscillation to determine how this parameter affects the microstructural uniformity and thermal behavior of the joints. Stainless steel 316L samples were exposed to molten solar salt at a constant temperature of 400 °C to simulate service conditions and evaluate the thermal stability of the welded regions. The molten salt mixture was formulated using sodium nitrate ($NaNO_3$, 99.5%) and potassium nitrate (KNO_3, 99.5%), both supplied by SQM (Antofagasta, Chile).

2.1 Materials

The plate used as the base material (BM) is a 316L austenitic stainless steel (ASS) measuring 250x150x6 mm. Its chemical composition is shown in Table 1.

Table 1 Stainless Steel grade AISI 316 L, composition, wt%

AISI	%C	%Mn	%Si	%Cr	%Ni	%Mo	%P	%S
316 L	0.039	1.14	0.393	16.54	10.30	1.99	0.024	0.0024
Norm	0.03	2.00	0.75	16-18	10-14	2-3	0.045	0.030

2.2 Welding process

In order to evaluate the behavior between both welding processes, two welding beads were made on a 250x150x6 mm AISI 316L steel plate (Fig. 1) with similar filler material ER316L, by means of a GMAW process with short circuit metal transfer with and without mechanical oscillation of the electric arc.

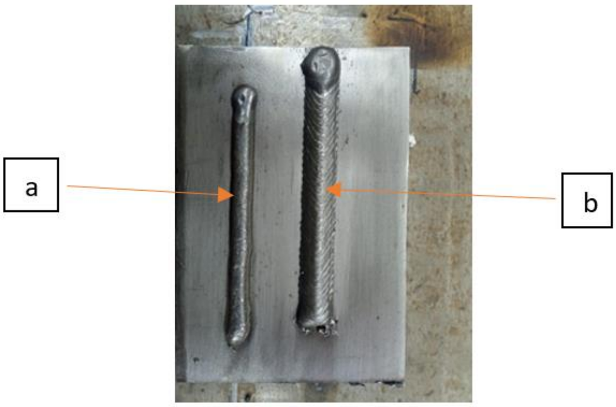

Figure 1 Weld beads (a) without oscillations; (b) with oscillations

The welding process was carried out using a Tartilope V4 CNC welder (Fig 2), with four degrees of freedom for the gun, generating the triangular oscillatory motion of an electric arc in one of the welds. The second weld was made without mechanical arc oscillation. This Tartilope V4 CNC equipment offers complete control and repeatability of parameters such as frequency, lateral dwell time, and oscillation amplitude.

A mixture of 80% argon and 20% carbon dioxide (80% Ar + 20% CO_2) was used as the shielding gas, with a fixed flow rate of 16 l/min, measured using a gas mixer. The gun was aligned vertically at 90° to the base metal (BM), allowing easy adjustment of the nozzle-to-work distance (TWD).

Figure 2: Welding CNC Tartilope V4 that applies the mechanical oscillation in the GMAW process

The welding parameters used are shown in Table 2. This matrix consists of wire speed, oscillation frequency, and oscillation type. From this, constant wire speeds of 4 m/s and an oscillating arc frequency of 1 Hz are used, as well as a non-oscillating arc. The parameters that were kept constant for the manufacture of both weld seams were determined from Table 1. The frequency used for the oscillating seam was 1 Hz, and 0 Hz for the non-oscillating weld (Table 2).

Table 2 Parameters used in both welded samples / welding beads

Oscillation Amplitude A (mm)	12
Reference Voltage Ur (V)	18
Oscillation Type	Triangular
Welding Speed (cm/min)	15
Shielding Gas Type	80% Ar + 20% CO_2
Flow Rate (l/min)	16
Welding Position	Flat
Transfer Type	Short Circuit
Nozzle-to-Work Distance DTP (mm)	15
Wire Type	AWS ER316L
Wire Diameter (mm)	1.2

3. Results

Metallography's obtained by oscillating arc, as shown in Figure 3, reveal smaller and more uniformly distributed dendrites than welds made without this method. The better distribution and smaller size of this constituent reduce the segregation of impurities, such as sulphur and phosphorus, at grain boundaries and the formation of delta ferrite and chromium carbides in these regions. This is because oscillation welding processes promote more uniform thermal dissipation, minimizing abrupt and localized thermal gradients, which in turn promotes more homogeneous nucleation of dendrites.

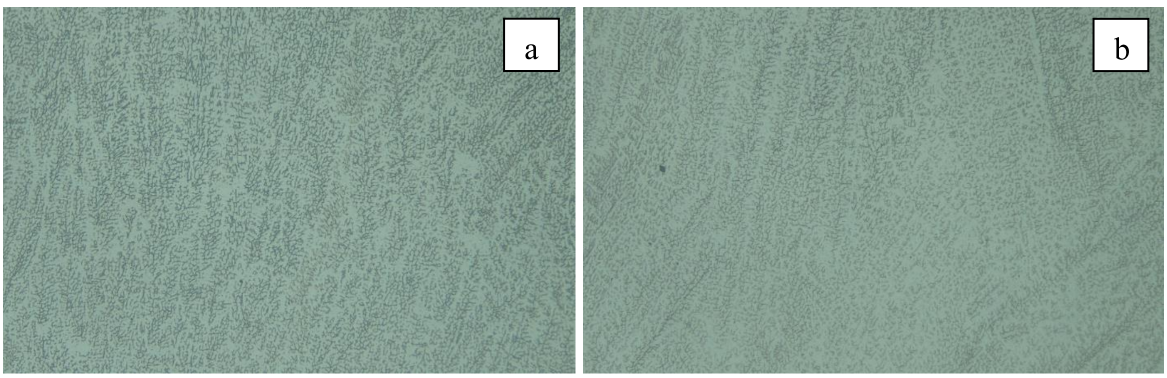

Figure 3. Metallography of 316L stainless steel welded coupons produced using different welding procedures: (a) with oscillation and (b) without oscillation

In figure 4 it is shown the mass loss of weld samples produced with and without oscillation after exposure to 120 h, 1000 h and 1500 h in a molten salt mixture (solar salt) at 400 °C. The results show a consistently lower mass loss for the oscillated welds, indicating better corrosion resistance. This improvement is attributed to a more uniform distribution of alloying elements such as chromium and nickel within the weld metal, promoted by the oscillatory arc movement. The oscillation also enhances local heat dissipation and preheating, leading to more homogeneous dendritic nucleation and solidification. Consequently, the formation of deleterious phases such as delta ferrite and chromium carbides at grain boundaries is minimized, reducing susceptibility to intergranular corrosion. Moreover, the oscillation process extends cooling times due to more controlled heat extraction, resulting in a finer and more stable microstructure. Altogether, the combination of homogeneous heat distribution, controlled cooling, and refined microstructure explains the superior mass stability of the oscillated welds which becomes more visible with a long-term molten salt exposure.

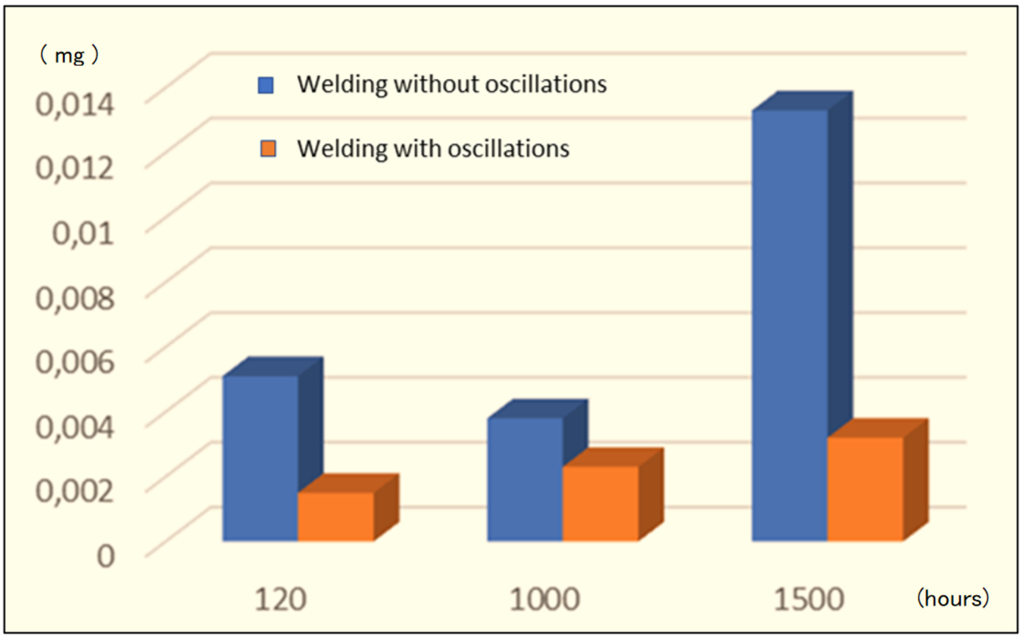

Figure 4: Loss of mass-produced using different welding procedures

To ensure a clear comparative understanding of the microstructural evolution of AISI 316L welds exposed to molten solar salt at 400 °C, SEM (Figure 5) analyses were performed across three representative zones: Zone 1 (Weld Pool), Zone 2 (Heat-Affected Zone, HAZ), and Zone 3 (Base Material). Figure 5 presents selected SEM micrographs comparing welded samples produced with and without mechanical arc oscillation after short-term exposure (120 h) and long-term exposure (1000 h and 1500 h). In the 120 h condition, Zones 1 and 2 in the oscillated welds display a more compact and uniform surface morphology, with reduced surface irregularities and fewer corrosion products, compared to their non-oscillated counterparts. These differences are attributed to enhanced thermal homogenization and a refined microstructure generated by oscillation-assisted grain fragmentation and heterogeneous nucleation. After 1500 h of exposure, the distinction becomes more pronounced. Oscillated welds maintain greater structural integrity, with fine grain structures and minimal signs of degradation across Zones 1 and 2. In contrast, non-oscillated welds exhibit clear signs of surface damage, including larger pits, more extensive corrosion product accumulation, and grain boundary attack—especially in the HAZ and weld pool regions. Zone 3, corresponding to the base material, remains relatively stable across both exposure times, confirming that microstructural changes are localized to the weld and HAZ regions and directly influenced by the welding process parameters.

These results reinforce the conclusion that mechanical arc oscillation during welding significantly improves the corrosion resistance and microstructural stability of stainless steel welds under prolonged exposure to molten salts, by mitigating thermal gradients and promoting grain refinement mechanisms. Such improvements are critical for enhancing the reliability of welded joints in high-temperature thermal storage systems.

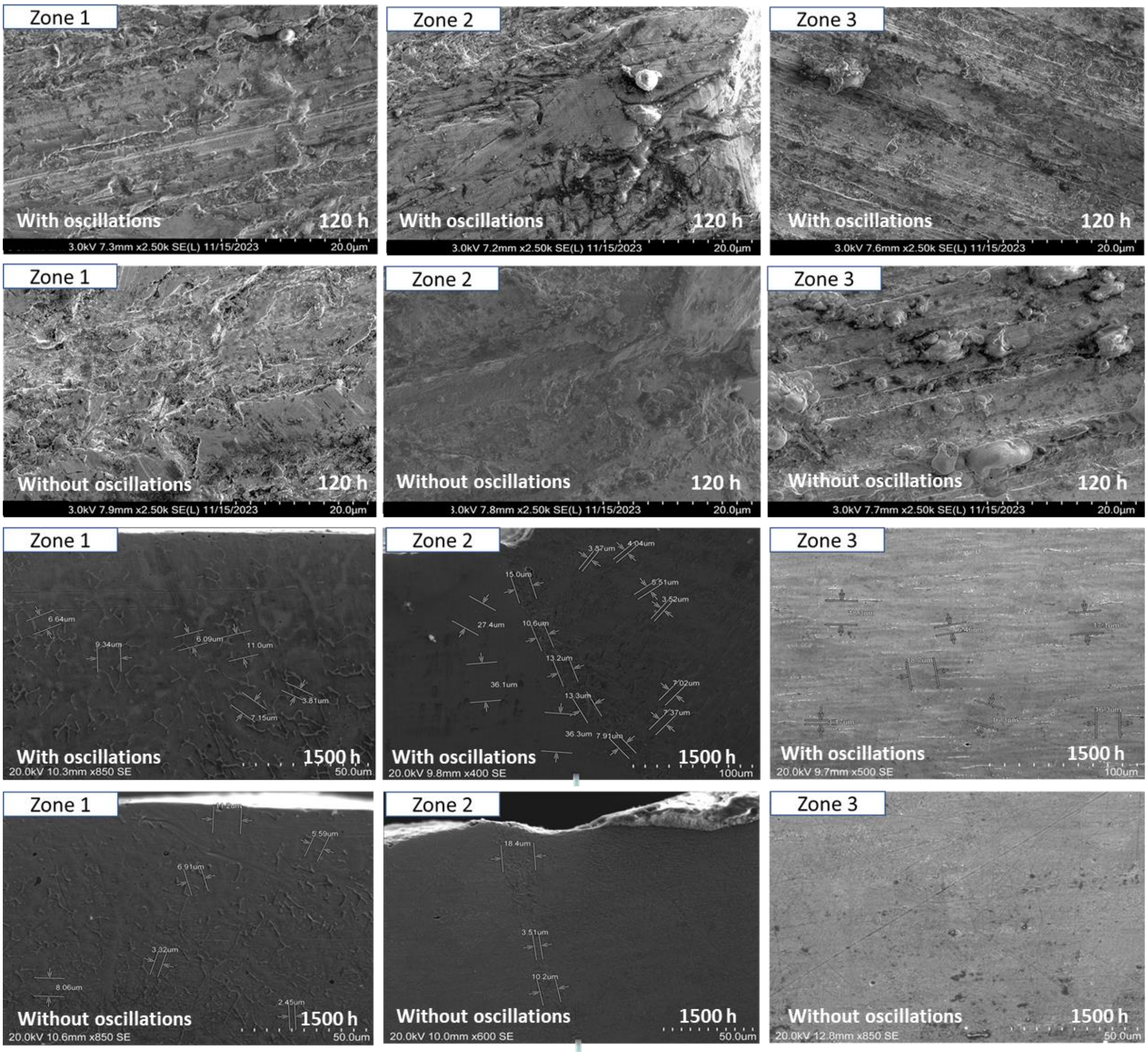

Figure 5: SEM for the weld sample with and without oscillations at 120 h and 1500 h of exposure with the molten salts

4. Conclusions

The results show that applying mechanical arc oscillation in the GMAW process significantly improves the microstructure and corrosion resistance of AISI 316L stainless steel welds exposed to molten solar salts at 400 °C. Oscillated samples exhibited lower mass loss, more refined and homogeneous microstructures, and reduced accumulation of corrosion products. This behavior is attributed to mechanisms such as dendrite fragmentation and heterogeneous nucleation, which promote the formation of dense and stable structures. The technique also reduces thermal stresses and enhances weld zone integrity. It is concluded that arc oscillation is an effective strategy to increase the durability of welded joints in thermal storage systems for CSP plants.

5. Acknowledgments

The authors are grateful for the support of ANID-Chile through the research projects, VIU24P0174, CONICYT/FONDAP 1523A0006 “Solar Energy Research Center” SERC-Chile, Engineering Project 2030 Code 16ENl2-71940 of Corfo, Government of Chile, and Grateful to Doctoral Program in Solar Energy Universidad de Antofagasta, Chile. Consortium of Engineering Faculties of the Antofagasta Region. ING 2030 Project Code 16ENI2-71940, CITMMUA Materials Engineering and Technology Center, VRIIP Strengthening Plan code ANT20992 and Minera Centinela 2024.

6. References

[1] G. Peiró, C. Prieto, J. Gasia, A. Jové, L. Miró, and L. F. Cabeza, “Two-tank molten salts thermal energy storage system for solar power plants at pilot plant scale: Lessons learnt and recommendations for its design, start-up and operation,” *Renew. Energy*, vol. 121, pp. 236–248, 2018, doi: 10.1016/j.renene.2018.01.026.

[2] A. Palacios, C. Barreneche, M. E. Navarro, and Y. Ding, “Thermal energy storage technologies for concentrated solar power – A review from a materials perspective,” *Renewable Energy*, vol. 156. Elsevier Ltd, pp. 1244–1265, Aug. 01, 2019. doi: 10.1016/j.renene.2019.10.127.

[3] S. Kuravi, J. Trahan, D. Y. Goswami, M. M. Rahman, and E. K. Stefanakos, “Thermal energy storage technologies and systems for concentrating solar power plants,” *Prog. Energy Combust. Sci.*, vol. 39, no. 4, pp. 285–319, 2013, doi: 10.1016/j.pecs.2013.02.001.

[4] A. Gil *et al.*, “State of the art on high temperature thermal energy storage for power generation. Part 1—Concepts, materials and modellization,” *Renew. Sustain. Energy Rev.*, vol. 14, no. 1, pp. 31–55, Jan. 2010, doi: 10.1016/j.rser.2009.07.035.

[5] M. Medrano, A. Gil, I. Martorell, X. Potau, and L. F. Cabeza, “State of the art on high-temperature thermal energy storage for power generation. Part 2—Case studies,” *Renew. Sustain. Energy Rev.*, vol. 14, no. 1, pp. 56–72, Jan. 2010, doi: 10.1016/j.rser.2009.07.036.

[6] F. Vilchez, F. Pineda, M. Walczak, and J. Ramos-Grez, “The effect of laser surface melting of stainless steel grade AISI 316L welded joint on its corrosion performance in molten Solar Salt,” *Sol. Energy Mater. Sol. Cells*, vol. 213, p. 110576, Aug. 2020, doi: 10.1016/j.solmat.2020.110576.

[7] E. González-Roubaud, D. Pérez-Osorio, and C. Prieto, “Review of commercial thermal energy storage in concentrated solar power plants: Steam vs. molten salts,” *Renewable and Sustainable Energy Reviews*, vol. 80. Elsevier Ltd, pp. 133–148, 2017. doi: 10.1016/j.rser.2017.05.084.

[8] J. D. Osorio *et al.*, “Failure Analysis for Molten Salt Thermal Energy Storage Tanks for In-Service CSP Plants Failure Analysis for Molten Salt Thermal Energy Storage Tanks for In-Service CSP Plants,” no. March 2024.

[9] M. Walczak, F. Pineda, A. G. Fernández, C. Mata-Torres, and R. A. Escobar, “Materials corrosion for thermal energy storage systems in concentrated solar power plants,” *Renew. Sustain. Energy Rev.*, vol. 86, 2018, doi: 10.1016/j.rser.2018.01.010.

[10] C. Suárez, A. Iranzo, F. J. Pino, and J. Guerra, “Transient analysis of the cooling process of molten salt thermal storage tanks due to standby heat loss,” *Appl. Energy*, vol. 142, pp. 56–65, 2015, doi: 10.1016/j.apenergy.2014.12.082.

[11] C. Prieto, R. Osuna, A. I. Fernández, and L. F. Cabeza, “Thermal storage in a MW scale. Molten salt solar thermal pilot facility: Plant description and commissioning experiences,” *Renew. Energy*, vol. 99, pp. 852–866, Dec. 2016, doi: 10.1016/j.renene.2016.07.053.

[12] H. Guo *et al.*, “Analysis of thermal and mechanical properties with inventory level of the molten salt storage tank in central receiver concentrating solar power plants,” *Appl. Therm. Eng.*, vol. 260, no. June 2024, p. 124984, 2025, doi: 10.1016/j.applthermaleng.2024.124984.

[13] Y. Hong, T. Pickle, Y. U. Zhenzhen, J. Vidal, and C. Augustine, “Impact of Plate Thickness and Joint Geometry on Residual Stresses in 347H Stainless Steel Welds,” *Weld. J.*, vol. 102, no. 11, pp. 279S-291S, 2023, doi: 10.29391/2023.102.021.

[14] C. Osorio, Julian D., Mehos, Mark, Martinek, Janna, Hamilton, Bill, Imponenti, Luca, Kelly, Bruce, Price, Hank, Yu, Zhenzhen, Ni, Chen, Rivera-Alvarez, Alejandro, Torres, Jose, and Nieto, “Modeling of Stress Distribution in Molten Salt Thermal Energy Storage Tanks for In-Service Central Receiver Power Plants,” *5th Therm. Energy Storage Work. 2-3 August 2023, San Antonio, Texas*, p. 627281636, 2023.